

Kinetics of subsurface hydrogen adsorbed on niobium: Thermal desorption studies

A.L. Cabrera^{a)} and J. Espinosa-Gangas

Facultad de Fisica, Pontificia Universidad Catolica de Chile, Casilla 306, Santiago 22, Chile

Johan Jonsson-Akerman and Ivan K. Schuller

Department of Physics, University of California at San Diego, La Jolla, California 92093-0319

(Received 25 January 2002; accepted 29 July 2002)

The adsorption/absorption of hydrogen and the adsorption of carbon monoxide by niobium foils, at room temperature, was studied using thermal desorption spectroscopy. Two hydrogen desorption peaks were observed with a maximum at 404 and 471 K. The first hydrogen desorption peak is regarded as hydrogen desorbing from surface sites while the second peak, which represents desorption from surface sites stronger bound to the surface, also has a component—due to its tailing to higher temperatures—of hydrogen diffusing from subsurface sites. Carbon monoxide adsorption was used to determine the number of surface sites, since it does not penetrate below the surface. Two carbon monoxide desorption peaks are observed in these experiments: at 425 and 608 K. The first peak is regarded as the adsorption of molecular carbon monoxide, and the second, as carbon monoxide dissociated on the niobium surface. The crystallographic orientation of the foils was determined by x-ray diffraction and showed a preferential (110) orientation of the untreated foil due to the effect of cold rolling. This preferential orientation decreased after hydrogen/heat treatment, appearing strong also in the (200) and (211) orientations. This change in texture of the foils is mainly due to the effect of heat treatment and not to hydrogen adsorption/desorption cycling. The kinetics of hydrogen and CO desorption is compared with that of Pd and Pd alloys.

I. INTRODUCTION

The interaction of hydrogen with metals is still a subject of current interest due to the potentially important applications that this research might generate. Areas of active technological development such as the chemical industry, hydrogen storage, hydrogen sensors, and magnetic recording, among others, might benefit from these studies in the near future.

Examples of research results in these areas that are closely related to future technological developments are the following:

(i) Gryaznov^{1,2} pioneered work on hydrogen diffusion through thin-walled pure metal membranes for catalytic applications. The facile permeation of hydrogen through palladium and palladium alloys suggests a number of applications in some chemical processes: the design of more efficient reactors³ for several hydrogenation or dehydrogenation reactions. Nevertheless, the feasibility of an industrial application (on a large scale) relies on reducing the reactors' cost since a reactor made of Pd would be extremely expensive.

(ii) Klose and co-workers^{4,5} have recently demonstrated a continuous reversible change in magnetic coupling between Fe and Nb layers induced by hydrogen absorption by Nb. These results are potentially useful in the development of hydrogen sensors.

The difference between Pd and Nb with regard to hydrogen adsorption is that hydrogen in Pd readily diffuses inside the bulk (this happens even at room temperature and subatmospheric pressures) until reaching a limiting concentration of 50%. Diffusivity of hydrogen in Nb is not so different than that in Pd;⁶ nevertheless the amount of hydrogen absorbed by Nb is controlled by the low solubility at equilibrium conditions.^{7,8}

Early studies of hydrogen adsorption by Nb were performed by Pryde and Titcomb.^{7,8} They studied the thermodynamics of hydrogen absorption by Nb filaments at low partial pressures of hydrogen (10^{-7} – 10^{-2} torr). They determined an expression for the hydrogen concentration in the metal in equilibrium at a given pressure. We calculated this concentration under our experimental conditions (exposures at 10^{-6} torr at temperatures around 343 K) and found that it is less than 0.8%. This means that the solubility in Nb is about 63 times less than in Pd. They also were able to obtain a desorption energy of about 14 kcal/mol.

^{a)}Address all correspondence to this author.

Pick *et al.*⁹ claimed that they were able to activate the Nb surface using a thin overlayer of Pd. According to their results they were successful in detecting large amounts of hydrogen diffusing into the Nb film at 455 K using change of film resistance techniques. They determined that the desorption energy of hydrogen from pure Nb foils was 25 kcal/mol, and this was decreased to 21.7 kcal/mol for Pd capped Nb foil. Later on, Pick¹⁰ reported a value of 14.8 kcal/mol for the desorption of hydrogen from recrystallized Nb foils with (110) orientation using the same kind of experiments. Strongin and his research group¹¹ mapped the Nb/H phases in thin 20-nm Nb films capped by 10-nm Pd film using x-ray diffraction (XRD). They claim the observation of a high density phase with 50% hydrogen concentration in Nb.

An attempt to describe the mechanism of hydrogen absorption by metals is based on the preferential surface or subsurface sites in the substrate that are occupied by hydrogen, determined by energy minimizing conditions imposed on the hydrogen/metal system. By definition, a subsurface site for hydrogen adsorption would be an interstitial site below the first layer of metal atoms. In fact, Rieder and co-workers¹² defined subsurface site in Pd(111) as an interstitial site between the first and second metal layers. But in the case of a metal surface structure not so closely compacted, like the orientation (110) for a face-centered-cubic (fcc) lattice or (100) for a body-centered-cubic (bcc) lattice, Rieder's definition of subsurface site becomes ambiguous.

We use a computer program developed by Van Hove and Hermann¹³ to represent the ideal surface structure of Nb(110) in Fig. 1(a) and Nb(100) in Fig. 1(b). Using this program, hydrogen and Nb atoms are drawn using their relative covalent radii. A hydrogen atom would be represented by a smaller sphere (represented in gray) than the Nb atoms and could fit an interstitial site. In Fig. 1(b) we represent sites on top of the first Nb layer as site 1 and between Nb atoms of the first layer—and on top of second Nb layer—as site 2. These are still surface chemisorption sites for use, while the interstitial site below the second Nb layer is a real subsurface site (site 3). Equivalent interstitial bulk sites below the third Nb layer are sites for hydrogen bulk diffusion.

The absorption of hydrogen by Pd was tentatively explained by Lagos,¹⁴ Lagos and Schuller,¹⁵ and Lagos *et al.*¹⁶ using the idea of a process mediated by subsurface bonding of hydrogen. According to their calculations, hydrogen would prefer to bind to subsurface sites rather than surface sites in Pd based on the energy required for the binding. The preferential absorption of hydrogen by these subsurface sites would facilitate hydrogen diffusion into the bulk of the metal.

Subsurface bound hydrogen in Nb was obtained by Romero *et al.*¹⁷ using molecular dynamic simulations. They obtained a value of 9.2 kcal/mol (0.4 eV/atom) for

preferential adsorption of atomic hydrogen at 0.25 nm below the Nb(100) surface. This site would correspond to an interstitial site between the second and third Nb atomic layer (equivalent to site 3 described above).

Experimental work reporting subsurface adsorption of hydrogen in Nb¹⁸ and in other metals such as Cu¹⁹ have also been published. Nevertheless, a significant difference between this subsurface adsorption in Nb and Pd is found: Pd easily absorbs large amounts of hydrogen at room temperature without further treatment (two hydrogen atoms for every four Pd atoms) while Nb does not. In the case of Nb the surface is blocked to hydrogen absorption by Nb oxide and requires to be cleaned adequately.

The purpose of our work is to determine if hydrogen is desorbing from site 1, 2, or 3 as defined in Fig. 1(b) using thermal desorption spectroscopy (TDS) and correlate these energies with crystallographic information of the

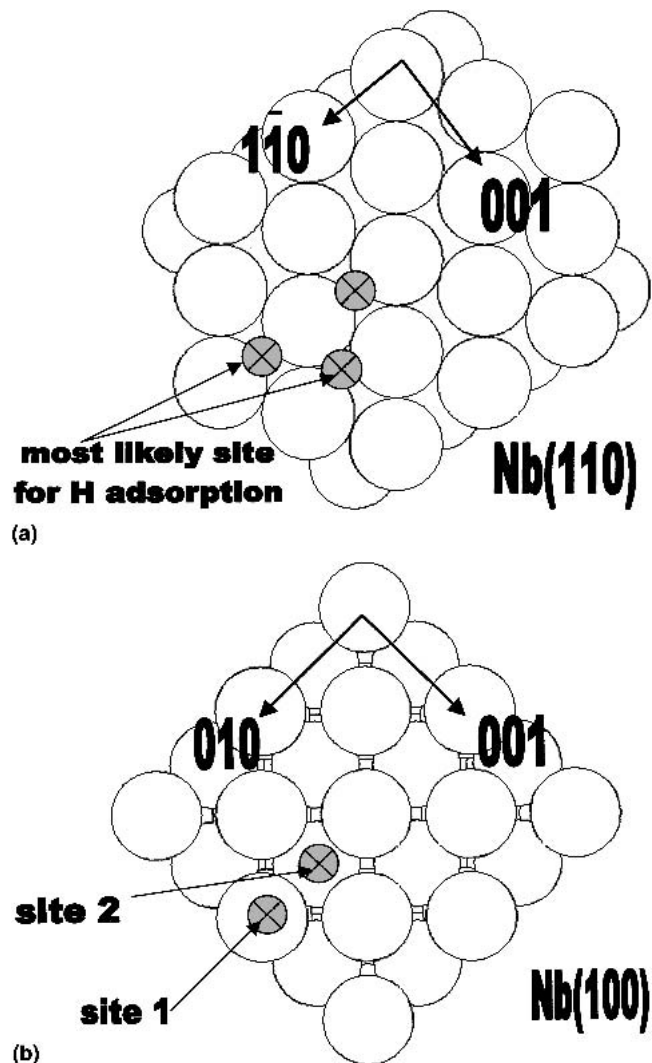


FIG. 1. Picture of the surface of an ideal Nb crystal oriented in the (a) (110) direction and (b) (100) direction. Sites 1 and 2 are possible places for hydrogen adsorption.

Nb surface structure obtained by XRD. Discussion about possible kinetic analysis of the TDS curves using a standard method described by various authors in review papers will be given. The interpretation of the desorption results will be compared with prior data on hydrogen adsorption by transition metal foils^{20,21} and from Pd, Ag–Pd, and Ru–Pd foils.²²

The study of the carbon monoxide adsorption by metal foils is also useful since CO does not penetrate the surface. A comparison between the hydrogen and CO signal intensity during desorption can give an indication of how much hydrogen is bound in subsurface sites.

There is also a significant amount of prior experimental work done by other authors for the H–Pd system which deals with surface interaction only,^{23–27} a weak bound subsurface state^{23,28,29} on single crystals of Pd, and bulk hydrogen diffusion in Pd.^{30–32} In addition, there is also experimental work to determine surface cleanliness of metallic surfaces using CO adsorption fingerprinting.^{33–35}

Understanding the mechanism of hydrogen adsorption/diffusion in Nb might lead to understanding why hydrogen easily diffuses inside Pd and not other metals, such as Ni and Co. This is important for developing hydrogen storage with less expensive metals than Pd.

II. EXPERIMENTAL

Samples of pure niobium (Nb) foil with approximate dimensions of $1.0 \times 1.0 \times 0.025$ cm were cut from a larger piece of foil obtained from Johnson Matthey, Ltd. (Ward Hill, MA), and mounted on the manipulator. The purity of the foils was 99.99%. The foils were spot-welded to two 0.09-cm diameter 316 stainless steel wires which were clamped on 0.32-cm copper bars of a sample manipulator. The temperature of the samples was monitored by a 0.0127-cm diameter chromel–alumel thermocouple spot-welded to one face of the foils. The sample was resistively heated using a high-current alternating current (ac) power supply.

A. Surface analyses

Surface cleanliness and surface elemental composition of the foils were monitored with Auger electron spectroscopy (AES) in an independent vacuum chamber with a base pressure of 1×10^{-5} torr.

AES analyses were performed with a cylindrical mirror analyzer from Physical Electronics using 2-keV electrons, 1×10^{-6} A beam current, and 2-V peak-to-peak modulation. The spectra were obtained by scanning from 100- to 1100-eV energy range. More details of this surface analysis system can be found elsewhere.^{20,21} The main surface contaminants were carbon (271 eV) and sulfur (150 eV). The samples had a thin native niobium oxide coating. A treatment was developed to eliminate

surface contaminants and the native oxide: the foils were subjected to several cycles of flash desorption to 973 K and Ar ion sputtering until a fresh niobium surface was observed by AES.

B. Thermal desorption analyses using the mass spectrometer

The manipulator was placed inside a custom-made vacuum system. The vacuum system mounted on a steel rack consisted of a small all-stainless steel chamber and a 50 l/s Alcatel turbomolecular pump (ATP80) backed with a Leybold Trivac S/D 1,6 B mechanical pump.

A stainless steel 6-way cross was a main part of the vacuum system and allows us to include the sample manipulator, an Ar ion sputtering gun, the quadrupole mass spectrometer (Dycor quadrupole gas analyzer), a Varian variable leak valve, and a glass view port. The base pressure of the system after outgassing stayed in the middle 10^{-9} torr. This system is described in detail elsewhere.³⁶

High-purity gases (at least 99.99%) from Matheson (AGA Chile) were used in all the experiments described in this work.

C. X-ray diffraction

XRD patterns of the foils were taken at room temperature with a Rigaku (Japan) diffractometer. The diffraction patterns were obtained with a Cu x-ray tube and a 2-circle goniometer in the usual θ – θ geometry. The x-ray tube was operated at a 9 kW on a rotating Cu anode, generating mainly Cu K_{α} radiation of 8.05 keV (0.154 nm). The goniometer was advanced between 5 and 140° at $0.02^{\circ}/s$ in the whole 2θ interval. The diffracted x-rays were detected with a solid-state detector. The diffraction patterns did not show any significant background signal.

III. RESULTS AND DISCUSSION

A. Hydrogen desorption from pure Nb foils

The foils were subjected to several cycles of flash desorption to 973 K, in vacuum, and Ar ion sputtering with the purpose of reducing contamination and surface oxide (without this treatment there was no hydrogen or CO adsorption). The foils were then exposed to 1000 l of H_2 at room temperature to perform the desorption experiments ($1 \text{ l} = 10^{-6}$ torr s).

After the dosing with gas, the foils were heated to 900 K at 5 K/s, and the desorbing gas was detected with the mass spectrometer. Typical spectra of hydrogen desorption from a piece of 1×1 cm of Nb foils after exposures of 1000 l are displayed in Fig. 2(a).

A broad peak of hydrogen, with a maximum at about 450 K, was detected. This broad peak can be deconvoluted mainly into two Gaussian curves using Origin 6.1.

One peak is located around 405 K, and the other around 471 K. The peak with a maximum located around 471 K is wider and tails to higher temperatures (approximately 550 K). Gdowski and collaborators³⁰ observed something similar for hydrogen desorbing from Pd: the shape of the hydrogen desorption spectrum for Pd(111) single crystals, after exposures to 630 l at subambient temperatures (around 261 K) already presented two desorption peaks. The first peak, observed around 350 K, corresponds to surface adsorption. The second peak, which shifted to higher temperatures (between 400 and 500 K) depending on the Pd temperature during dosing, corresponded to subsurface adsorption. For higher Pd temperatures (298 K) during exposure, a broad peak with a maximum at 800 K was identified with hydrogen in solid solution.

The hydrogen desorption from Nb is also similar to the case of hydrogen desorption from 5% Ru–Pd alloy that we studied earlier:³⁷ the broad peak centered around

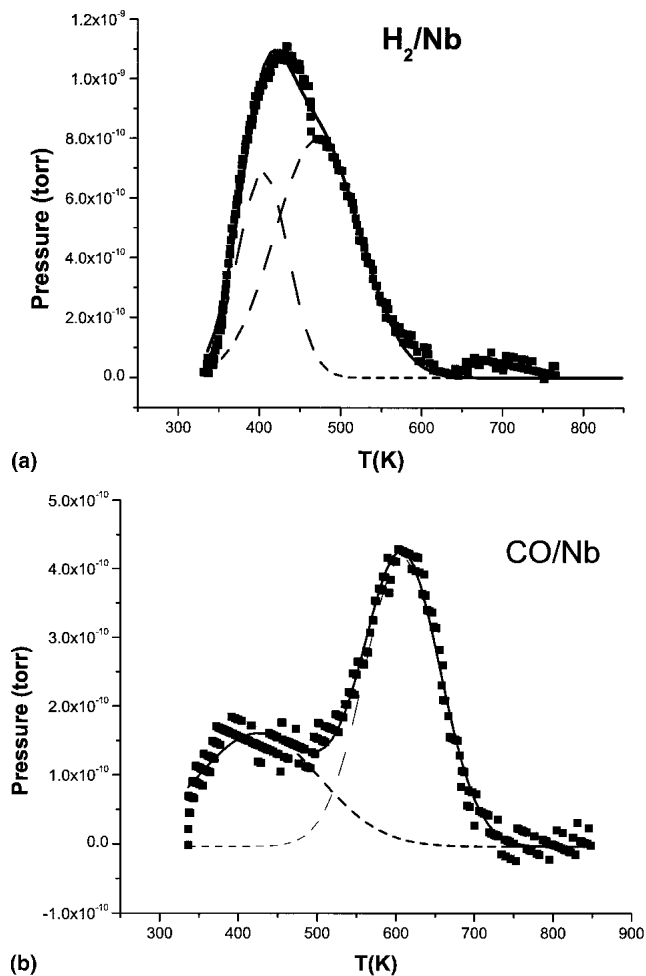


FIG. 2. (a) TDS spectra for H_2 desorption from pure Nb foils after exposure to 1000 l of H_2 and using a heating rate of 5 K/s. (b) TDS spectra for CO desorption from pure Nb foils after exposure to 1000 l of CO and using a heating rate of 5 K/s.

450 K was deconvoluted into two peaks of hydrogen desorption. The first peak is centered at about 413 K, and the second peak, at 525 K. The interpretation of the data is the same as in the case of Pd: the first peak is surface hydrogen, and the second peak is diffused hydrogen. This small percent of Ru alloying Pd significantly blocked the surface to hydrogen diffusion into the bulk of the metal. The hydrogen desorption from Nb is compared with the desorption from 5% Ru–Pd and 17% Ag–Pd alloys and from pure Pd in Fig. 3. Notice that the desorption from Ru–Pd and Ag–Pd was amplified 33 times compared to that from pure Pd, and the desorption of hydrogen from Nb was amplified by a factor 272. This graph highlights the deep hydrogen diffusion observed in pure Pd.

B. Carbon monoxide desorption from pure Nb foils

After the cleaning procedures already described in Sec. III, A, the foil was then exposed to 1000 l of CO at room temperature to perform the desorption experiments.

After the dosing with the gas, the foils were heated to 900 K, at 5 K/s, and the desorbing gas was detected with the mass spectrometer. Typical spectra of carbon monoxide desorption from a piece of 1×1 cm of Nb foils after exposures of 1000 l are displayed in Fig. 2(b). One can observe the appearance of two peaks: one at 425 K and the second at around 608 K. The shape of the first peak is not well defined due to background subtraction. The interpretation of the CO adsorption nature at each site according to well established evidence from experiments in other transition metals is the following: the first peak is desorption of molecular adsorbed CO. The second peak is related to dissociative adsorption. Nakamura

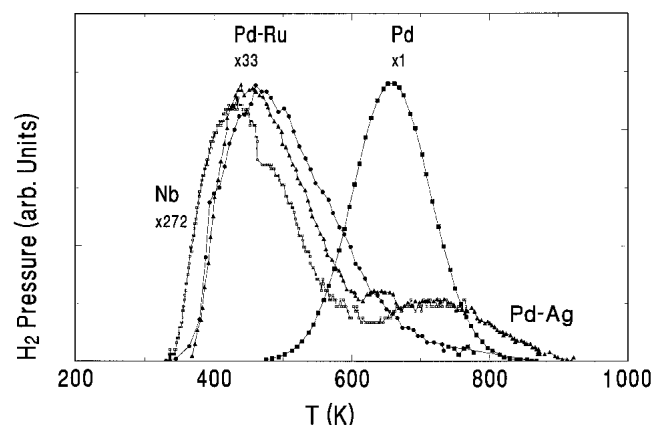


FIG. 3. TDS spectra for H_2 desorption from pure Nb (full circles), 5% Ru–Pd (open circles–squares), and 17% Ag–Pd (full triangles) alloys and from pure Pd (full squares) foils after exposure to 1000 l of H_2 and using a heating rate of 10 K/s (except for Nb in which case we used 5 K/s).

*et al.*³⁸ observed a shift of the x-ray photoelectron spectroscopy C 1s line attributed to adsorbed CO on polycrystalline Co. The shift occurred around 353 K and corresponded to a change from molecular CO to dissociated CO. This temperature corresponds to the temperature at which we exposed our Nb samples to CO. Moreover, the positions of the peaks, in the temperature scale, are very similar to CO desorbing from cobalt foil,³⁹ from single-crystal Fe(100),⁴⁰ and from single-crystal Ni with steeped surface.⁴¹ The area under the CO curve [Fig. 2(b)] is about 1/2 the area of the hydrogen curve [Fig. 1(b)]. This area is proportional to the initial gas coverage on the surface of Nb since CO remains only on the surface. Therefore, the amount of hydrogen adsorbed is not much larger than the amount of CO adsorbed, considering that the ionization cross section for H₂ is twice as large as that for CO. This is an indication of poor hydrogen diffusion into the bulk of Nb.

C. X-ray characterization of the foils

The XRD data obtained for the Nb foils before and after the experiments suggest that the microstructure of the Nb foil changes due to the heat treatment.

Initially, the foils are preferentially oriented in the (110) direction [with some components in the (200), (211), and (310) directions]. After hydrogen absorption at room temperature and heating the foils to 900 K in vacuum to perform desorption, the diffraction pattern changed; the (200) and (211) orientation became more prominent in comparison with the (110) orientation. Finally, the diffraction pattern obtained from a foil heated in vacuum up to 900 K but not exposed to hydrogen was obtained. The heat treatment alone made the (200) line become noticeably stronger in comparison with the (110) orientation.

Calculation of lattice parameter for Nb from the three XRD patterns showed no significant change from 0.330 nm. This is an indication that any change that occurred in the Nb foil due to the adsorption of hydrogen was localized at most on the very top surface.

D. Calculation of desorption energies

Activation energy for TDS desorption corresponding to a single peak can be obtained in two ways:

(i) The first method is using a simplified Redhead's formula.⁴² The preexponential factor is assumed, and the activation energy can be calculated from the following expression:

$$E = RT_p \{ \ln(\nu_n T_p / \beta) - 3.35 \} \quad (1)$$

In this case T_p is the temperature corresponding to the maximum of the desorption curve.

(ii) The second method is by plotting the logarithm of the rate constant versus the inverse absolute temperature. The kinetic parameters such as the desorption energy, the attempt frequency, and the order of the desorption can be obtained. The rate constant k appears in the rate equation for desorption:

$$dN/dt = -kN^n \quad (2)$$

where dN/dt is the rate of desorption, N is the concentration of adsorbed gas, and n is the order of the desorption process. The rate constant k normally obeys an Arrhenius-type rate law of the form:

$$k = \nu_n \exp(-E/RT) \quad (3)$$

where E is the desorption energy. This analysis is basically a numerical calculation of the rate constant. Nevertheless, when applied to our TDS it gives unreasonable values for the desorption energy and specially for the attempt frequency ν_n .

King⁴³ discussed in his thermal desorption review that the value of the activation energy is not so different even if $n = 1$ or $n = 2$ or if the heating rates vary from 1 to 1000 K/s when using Eq. (1). The dominant feature in Redhead's equation is the attempt frequency ν_n . The value of this frequency is well accepted⁴⁴ to be on the order of 10^{13} s^{-1} since it represents the vibration frequency of atoms or molecules attached to a surface held

TABLE I. Comparison of desorption data of H₂ and CO from different metal foils studied. The desorption energy is calculated from Redhead's formula which appears in Eq. (1), assuming an attempt frequency of 10^{13} s^{-1} .

Metal foil	Heating rate (K/s)	Surface H		Subsurface H		Molecular CO		Dissociated CO	
		T_p (K)	E (kcal/mol)	T_p (K)	E (kcal/mol)	T_p (K)	E (kcal/mol)	T_p (K)	E (kcal/mol)
Pd	10	650	39.8	375	22.5
						469	28.7		
5% Ru-Pd	10	413	24.9	525	31.9	No data taken		No data taken	
Nb	5	404	24.9	~550	34.2	425	26.2	608	38.0
		471	29.2						
Ni	12	420	25.0	...		378	22.6	570	34.5
		480	29.0						
Co	10	396	22.2	...		388	24.8	621	38.0
		475	28.8						

at temperature T . The value can be estimated by $k_B T/h$, where k_B is the Boltzman constant and h is the Planck constant.

We used Eq. (1) to calculate the desorption energy of H_2 and CO from Nb and compared it with the case of desorption from Pd and 5% Ru/Pd. These energies, the temperature value of the peaks (T_p), and the heating rates are listed in Table I. The energies of desorption are calculated by assuming an attempt frequency of 10^{13} s^{-1} . If no other assumption is taken, the desorption energy is an increasing function of the temperature using Eq. (1).

We also used scheme ii to obtain activation energies and order of the desorption. Since H_2 molecules dissociate on the surface of transition metals, the order n taken as two in the analysis is plausible, but the order n is determined by the best fit of the data to a straight line in an Arrhenius plot. Straight lines for the Arrhenius plots in the case of hydrogen desorption from Nb were obtained using $n = 2$ for both peaks. The slope of the lines in these plots yields activation energies corresponding to 9.9 ± 0.5 and 6.5 ± 0.5 kcal/mol for the first and second peaks, respectively. The energy values obtained for the first and the second peaks are in agreement with the values reported in our prior work on Pd, 5% Ru–Pd, and 17% Ag–Pd³⁷ using the same data analyses, but it seems that this data processing is the less reliable method. The energy values are always lower at least by a factor of two, but the most worrisome result is that the resulting attempt frequency is as low as 10^5 s^{-1} in some cases.

Something important to mention about this data processing is that in the case of hydrogen desorbing from Pd the Arrhenius plot can be fitted to a straight line only if $n = 1.25$ (fractional order for desorption). Explanation of fractional order for hydrogen desorption from subsurface sites in Pd can be qualitatively explained with the argument given below. In the case of dissociative adsorption, the order can be $n = 1$ if desorption proceeds from the recombination of immobile neighboring atoms. In principle, the order should be $n = 2$ since there is some degree of surface diffusion before recombination. If the order is fractional between 1 and 2, the surface hydrogen atoms are quickly replaced by atoms diffusing from the bulk; thus, the surface hydrogen concentration always remains high during desorption. Then, in this case, hydrogen desorption proceeds for the most part by the recombination of two neighboring immobile hydrogen atoms.

IV. CONCLUSIONS

One broad peak of hydrogen desorption at about 450 K is observed for Nb after exposure to hydrogen gas at around room temperature. A deconvolution of this curve shows that it is composed of a lower temperature peak associated with surface adsorption and a higher

temperature peak which contains a component of subsurface adsorption. Hydrogen adsorbed at the surface would desorb first before hydrogen absorbed in subsurface sites. The values of the “apparent” desorption energies obtained in these experiments (25–29 kcal/mol) are larger than the energy measured for bulk diffusion (2.4 kcal/mol) in Ref. 6 indicating that the rate-limiting step for desorption is the release of hydrogen from the surface sites.

ACKNOWLEDGMENTS

This research was partially supported by grants from the Chilean Government (FONDECYT 1000535), Fundacion Andes, and the United States Department of Energy. We thank Dr. Antonio Zarate and Dr. Jurgen Baier for performing surface analyses.

REFERENCES

1. V.M. Gryaznov, *Vestn. Adad. Nauk SSSR* 21 (1986).
2. V.M. Gryaznov, *Platinum Met. Rev.* **30**, 68 (1986).
3. J. Shu, B.P.A. Grandjean, A. Van Neste, and S. Kaliaguine, *Can. J. Chem. Eng.* **69**, 1036 (1991).
4. F. Klose, Ch. Rehm, D. Nagengast, H. Maletta, and A. Weidinger, *Phys. Rev. Lett.* **78**, 1150 (1997).
5. Ch. Rehm, H. Fritzsche, H. Maletta, and F. Klose, *Phys. Rev. B* **59**, 3142 (1999).
6. J. Volkl and G. Alefeld, in *Topics in Applied Physics: Hydrogen in Metals*, edited by G. Alefeld and J. Volkl (Springer Verlag, Berlin, Germany, 1978).
7. J.A. Pryde and C.G. Titcomb, *Solid State Phys.* **238**, 1293 (1972).
8. J.A. Pryde and C.G. Titcomb, *Solid State Phys.* **238**, 1301 (1972).
9. M.A. Pick, J.W. Davenport, M. Strongin, and G.J. Dienes, *Phys. Rev. Lett.* **43**, 286 (1979).
10. M.A. Pick, *Phys. Rev. B* **24**, 4287 (1981).
11. G. Reisfeld, N.M. Jisrawi, M.W. Ruckman, and M. Strongin, *Phys. Rev. B* **53**, 4974 (1996).
12. K.H. Rieder, M. Baumberger, and W. Stocker, *Phys. Rev. Lett.* **51**, 1799 (1983).
13. M.A. Van Hove and K. Hermann, *Surface Architecture and Lattice, a PC-based program*, Version 2.0 and later Versions (Lawrence Berkeley National Laboratory, Berkeley, CA, 1988).
14. M. Lagos, *Surf. Sci. Lett.* **122**, L601 (1982).
15. M. Lagos and I.K. Schuller, *Surf. Sci.* **138**, L161 (1984).
16. M. Lagos, G. Martinez, and I.K. Schuller, *Phys. Rev. B* **29**, 5979 (1985).
17. A. Romero, I.K. Schuller, and R. Ramirez, *Phys. Rev. B* **58**, 15904 (1998).
18. Y. Li, J.L. Erskine, and A.C. Diebold, *Phys. Rev. B* **34**, 5951 (1986).
19. K.H. Rieder and W. Stocker, *Phys. Rev. Lett.* **57**, 2548 (1986).
20. A.L. Cabrera, *J. Vac. Sci. Technol. A* **8**, 3229 (1990).
21. A.L. Cabrera, *J. Vac. Sci. Technol. A* **11**, 205 (1993).
22. A.L. Cabrera, E. Morales, J. Hansen, and I.K. Schuller, *Appl. Phys. Lett.* **66**, 1216 (1995).
23. H. Conrad, G. Ertl, and E.E. Latta, *Surf. Sci.* **41**, 435 (1974).
24. R.J. Behm, K. Christmann, and G. Ertl, *Surf. Sci.* **99**, 320 (1980).
25. M.G. Cattania, V. Penka, R.J. Behm, K. Christmann, and G. Ertl, *Surf. Sci.* **126**, 382 (1983).
26. C. Nyberg, L. Westerlund, L. Jonsson, and S. Andersson, *J. Electron Spectrosc. Relat. Phenom.* **54/55**, 639 (1990).

27. J-W. He and P.R. Norton, *Surf. Sci.* **195**, L199 (1988).
28. J.F. Lynch and T.B. Flanagan, *J. Phys. Chem.* **77**, 2628 (1973).
29. R.J. Behm, V. Penka, M.G. Cattania, K. Christmann, and G. Ertl, *J. Chem. Phys.* **78**, 7486 (1983).
30. G.E. Gdowski, T.E. Felter, and R.H. Stulen, *Surf. Sci.* **181**, L147 (1987).
31. W. Auer and H.J. Grabke, *Ber. Bunsen-Ges Phys. Chem.* **78**, 58 (1974).
32. B.D. Kay, C.H.F. Peden, and D.W. Goodman, *Phys. Rev. B* **34**, 817 (1986).
33. R.J. Behm, K. Christmann, G. Ertl, M.A. Van Hove, P.A. Thiel, and W.H. Weinberg, *Surg. Sci.* **88**, L59 (1979).
34. R.J. Behm, K. Christmann, G. Ertl, and M.A. Van Hove, *J. Chem. Phys.* **73**, 2984 (1980).
35. A. Noordermeer, G.A. Kok, and B.E. Niuwenhuys, *Surf. Sci.* **165**, 375 (1986).
36. A.L. Cabrera, E. Morales, L. Altamirano, and P. Espinoza, *Rev. Mex. Fis.* **39**, 932 (1993).
37. A.L. Cabrera, E. Morales, and J.N. Armor, *J. Mater. Res.* **10**, 779 (1995).
38. J. Nakamura, I. Toyoshima, and K. Tanaka, *Surf. Sci.* **201**, 185–194 (1988).
39. A.L. Cabrera, W.H. Garrido, and U.G. Volkmann, *Catal. Lett.* **25**, 115 (1994).
40. M.L. Burke and R.J. Madix, *Surf. Sci.* **273**, 20–34 (1990).
41. W. Erley and H. Wagner, *Surf. Sci.* **74**, 333–341 (1978).
42. P.A. Redhead, *Vacuum* **12**, 203 (1962).
43. D.A. King, *Surf. Sci.* **47**, 384 (1975).
44. D. Menzel, *Chem. Phys. Solid Surf.* **20**, 389 (1972).